Photochemical Reaction of Ozone and Dimethylacetylene: An Infrared Matrix Isolation and ab Initio Investigation

James K. Parker and Steven R. Davis*

Department of Chemistry, University of Mississippi, University, Mississippi 38677

Received: June 9, 1999

The photolysis of Ar/ozone/dimethylacetylene matrices (200/1/1) at $\lambda \geq 280$ nm and 12 K yields the following stable products: dimethylketene, the E and Z configurational isomers of methyl vinyl ketone, butane-2,3-dione, and acetic anhydride. The reaction of $O(^3P)$ with dimethylacetylene to form products of molecular formula C_4H_6O, including dimethyloxirene, was modeled using the second-order perturbation and CCSD(T) theories. In all cases, it is concluded that spin crossing takes place early on the reaction surface to take advantage of low singlet state activation barriers. The formation of butane-2,3-dione from singlet state O_2 molecules and dimethylacetylene, as well as the photolysis of DMA/O_3 reactant pairs, is discussed.

I. Introduction

The reaction of atomic oxygen with small, unsaturated hydrocarbons belongs to an important class of reactions due to its occurrence in combustion processes,[1] atmospheric reactions,[2] and biological systems.[3] The oxygen atom−acetylene reaction in solid argon has been found to yield ketene exclusively.[4] In related work, Bodot[5,6] and co-workers studied the photoinduced decomposition of 3-diazobutane-2-one in solid, inert gas matrices using infrared spectroscopy. They found dimethyloxirene as a product, as well as methyl vinyl ketone and dimethylketene.

While oxirenes are postulated[6−8] to be intermediates in the Wolff rearrangement,[9,10] until the Bodot study only perfluorodimethyloxirene had been spectroscopically observed.[11,12] Intrigued by this, we have examined the reaction of dimethylacetylene (DMA) and $O(^3P)$ in argon matrices at 12 K in order to determine whether dimethyloxirene could be isolated under these conditions. This reaction is fundamentally different than the photolysis of 3-diazobutane-2-one in that the initial product of photolysis of a diazoketone is a singlet ketocarbene, while addition of a triplet state oxygen atom to DMA leads to ground state triplet ketocarbene. Nevertheless, the initially formed triplet ground state can be promoted to the singlet state ketocarbene during photolysis.[13] It is singlet ketocarbene which undergoes Wolff rearrangement.[14]

The original goal of the present research was to determine whether dimethyloxirene could be observed from the reaction of oxygen atoms with DMA in an argon matrix at 12 K. However, the photolysis of ozone[15] leads to the production of $O_2(^3\Sigma_g^-)$, $O_2(^1\Sigma_g^+)$, and $O_2(^1\Delta_g)$ molecules in addition to $O(^3P)$ and $O(^1D)$ atoms; consequently, we have been able to observe products of the following molecular formulas: C_4H_6O, $C_4H_6O_2$, and $C_4H_6O_3$. Therefore, this study is concerned not only with the oxygen atom addition to DMA but also with oxygen molecule and ozone molecule reactions with DMA.

II. Experimental Section

Dimethylacetylene (99%, Aldrich) was freed of relatively volatile impurities by three consecutive freeze−pump−thaw cycles at liquid nitrogen temperature. Upon warming to room temperature, DMA vapors were expanded into an evacuated sample chamber and diluted with argon (99.995%, Air Products) to an Ar/DMA mole ratio of 100/1. Normal ozone, $^{16}O-^{16}O-^{16}O$, and the isotopically pure $^{18}O-^{18}O-^{18}O$ ozone were obtained by passing an electric discharge, from a Tesla coil, through a sample of oxygen gas (99.996%, Air Products; ^{18}O isotope from Eurisotop, 98.01% enrichment) contained in a glass U tube which was submerged in liquid nitrogen. The ozone deposited onto the walls of the tube as it formed. The solid ozone was freed of residual oxygen molecules by pumping at 77 K. The purified ozone was then warmed to room temperature, expanded into a separate evacuated sample chamber, and diluted with argon to an Ar/O_3 mole ratio of 100/1. Matrices containing methyl vinyl ketone, butane-2,3-dione (both 99%, Aldrich), and acetic anhydride (>98%, Fluka) were prepared in the same manner as the DMA matrix. The IR spectrometer and accompanying vacuum chamber have been described in detail elsewhere.[16] The DMA/Ar and ozone/Ar gas mixtures were co-deposited on a gold-mirrored matrix support at a combined rate of 8.4 mmol/h for a total of 24.2 mmol. The matrix support was held at 12 K with a closed-cycle, single-stage helium refrigerator (APD Cryogenics, model DE-202). The temperature was measured at the cold plate with a gold/calomel thermocouple. All infrared spectra were recorded using a Nicolet 740 FTIR spectrometer operating at 1 cm^{-1} resolution with data spacing in 0.121 cm^{-1} intervals. After recording the initial spectrum (number of scans is 128 for all spectra), the matrices were subjected to the photolyzing radiation of a 200 W Hg−Xe arc lamp (lamp model UXL 200H Hg Xe by Ushio and model A 1010 lamp housing by Photon Technology International). The radiation was filtered through a 51 mm water cell and then a 280 nm Hoya cut off filter before coming in contact with the matrix sample. The temperature of the matrix sample did not rise above 14 K during any photolysis interval, unless otherwise noted. All matrix spectra were successively photolyzed at precise time intervals.

The ab initio calculations were performed using the Gaussian 94 suite of programs[17] running on either a Cray C98/8512 or a Silicon Graphics Power Challenge computer. All structures were optimized using second-order Moller−Plesset perturbation

10.1021/jp991880a CCC: $18.00
Published on Web 08/21/1999

theory[18] with the 6-31+G(d,p) basis,[19−22] unless otherwise noted. Analytic gradients were used in the geometry optimizations with valence shell electrons correlated. All stationary points were verified to be true minima or transition states by calculation of normal vibrational modes using the analytic second derivative method in the harmonic approximation. Zero-point vibrational energies (ZPE) were added to the electronic potential energies to obtain relative energies at 0 K. Single-point energies at the CCSD(T)/6-31+G(d,p) level[23−27] were carried out on all MP2-optimized minima and transition states.

III. Results

DMA in the Ar matrix (Ar/DMA = 200/1) at 12 K displayed IR absorption bands at 2975.9 (s), 2936.2 (vs), 2873.1 (s), 2741.7 (m), 2057.4 (w), 1447.6 (vs), 1407.9 (w), 1405.5 (w), 1379.4 (m), 1157.3 (w), 1131.6 (w), 1040.0 (m), and 1035.1 (m) cm^{-1} where vs, s, m, and w stand for very strong, strong, medium, and weak bands, respectively. The photostability of DMA was tested by irradiation of the matrix with photons of $\lambda \geq 280$ nm and revealed no new IR bands; filterless irradiation increased the matrix temperature to about 30 K but did not result in any new product bands, in agreement with an earlier study.[28] When DMA was isolated in an argon matrix containing ozone (Ar/DMA/ozone = 200/1/1), the absorption bands of DMA shifted to the following: 2976.2, 2936.7, 2872.5, 2740.9, 2056.5, 1447.2, 1407.1, 1404.3, 1378.9, 1157.9, 1131.1 cm^{-1}. These shifts could be due to the different matrix environment, or formation of a weak DMA−ozone complex, or both. The 1040−1035 cm^{-1} bands of DMA were obscured by ozone absorption in this region.

Table 1 lists all product band frequencies, assignments, and relative intensities resulting from photolysis of a 200/1/1:Ar/DMA/ozone matrix using the filtered radiation ($\lambda \geq 280$ nm) of a medium-pressure Hg−Xe arc lamp. The reaction was studied using the $^{16}O-^{16}O-^{16}O$ and $^{18}O-^{18}O-^{18}O$ isotopomers of ozone; standard DMA was used in all experiments. The following species are products of the ozone−DMA photolysis reaction: dimethylketene (DMK), ketene, acetic anhydride (AAH), butane-2,3-dione (BDN), methyl vinyl ketone (MVK), CO_2, and CO. Dimethylketene,[6,29] ketene,[30] and CO[31] band assignments were made by comparison of our matrix infrared spectra with argon matrix and gas phase spectra available in the literature. Methyl vinyl ketone, butane-2,3-dione, and acetic anhydride band assignments were made by comparison of product bands from the photolysis reaction with their argon matrix IR spectra (M/R = 1000/1) obtained in this laboratory.

Figure 1 shows the photolysis−time dependence of the absorbance spectra of product bands in the 2100 and 1700 cm^{-1} regions. In Figure 1A, spectrum a was taken immediately prior to the first photolysis. The doublet near 2110 cm^{-1} is due to ozone. As photolysis time increases, this doublet decreases in intensity with simultaneous appearance of product bands near 2130 cm^{-1}, which increase in intensity with photolysis time. The strong doublet near 2130 cm^{-1}, as well as the 2119 cm^{-1} band, are due to dimethylketene. Figure 1B shows the product bands in the 2100 cm^{-1} region when the $^{18}O-^{18}O-^{18}O$ isotopomer of ozone is the photolytic precursor. The product bands have shifted to lower wavenumber and their relative intensities have changed. The three bands between 2100 and 2110 cm^{-1} are due to dimethylketene. Figure 1, C and D, shows the product band absorptions of molecules with carbonyl functional groups. The most intense band in Figure 1C, at 1722 cm^{-1}, is due to butane-2,3-dione. The band at 1720 cm^{-1} is due to (*Z*)-methyl vinyl ketone and the doublet near 1700 cm^{-1} is due to (*E*)-methyl vinyl ketone. It is interesting to note that the intensity ratio, *I*(1720)/*I*(1700), of these two carbonyl bands of methyl vinyl ketone decreases slightly during the course of photolysis, from 1.40 to 1.30. Ar matrices containing 0.1% MVK, which have been prepared from the room temperature gases, have a *I*(1720)/*I*(1700) ratio of 0.30, which rises to 0.66 when exposed to the 280 nm filtered radiation of the arc lamp for 30 min; these configurational isomers readily interconvert at these wavelengths.

IV. Discussion

Products of C_4H_6O Composition. The first part of the discussion will focus on the $O(^3P)$ atom addition reaction to dimethylacetylene. We have modeled this reaction using the MP2/6-31G(d,p) level of theory; the results of which are presented in Figure 2 as an energy vs C−O bond length plot. The data in the plot were generated in the following way: the O atom of the C−O bond of fully optimized triplet (*Z*)-dimethylketocarbene ((*Z*)-DMKC) was stepped away from the carbonyl carbon in 0.10 Å intervals while optimizing all other coordinates at each step point; at C−O = 1.8537 Å, a transition state was observed. The MP2 activation energy of 8.0 kcal/mol for this reaction (Table 4) was calculated by placing $O(^3P)$ 15 Å away from fully optimized singlet DMA and subtracting the resulting electronic and zero-point vibrational energies (ZPE) of this triplet state system from the sum of the electronic and ZPE energies of the transition state. The energy of this system changes by only 0.031 kcal/mol when the $O(^3P)$−C distance of DMA is decreased from 15 to 2.4069 Å, indicating that the interaction energy between DMA and $O(^3P)$ is negligible even at this relatively small distance. Referring again to Figure 2, we find that the reaction is exothermic by 51.4 kcal/mol, when the ZPE's of reactants and products are included. Therefore, the ground state triplet ketocarbene is formed hot with approximately 51 kcal/mol of excess energy which can be channeled into excited vibrational states and, eventually, dissipated by the matrix. However, as noted from its absence in Table 1, we observed no ketocarbene product in the infrared matrix spectra. Therefore, the vibrationally excited triplet state ketocarbene must undergo rapid intersystem crossing to form the observed products of C_4H_6O composition. Calculated singlet and triplet activation energies in Tables 3 and 4 provide ample evidence in support of this conclusion.

We now consider the formation of singlet state dimethylketene (DMK) from hot triplet state (*Z*)-DMKC. Plotted in Figure 3 is a potential energy diagram, computed from second-order perturbation theory, for the thermal rearrangement of triplet state (*Z*)-DMKC to triplet state DMK, and for the thermal rearrangement of singlet DMKC to singlet state DMK. These potential energy diagrams were generated by finding the transition state which connects the products of interest and using the intrinsic reaction coordinate (IRC) option in Gaussian 94 to follow the imaginary modes back to the products. The activation energy (Table 4) along the triplet surface is a considerable 57.3 kcal/mol, whereas the activation energy along the singlet surface is only 1.9 kcal/mol. It is clear from energetics alone that in order to form ground state DMK, this species must undergo intersystem crossing without passing through the triplet transition state. Singlet DMKC, a molecule that exists without the E/Z conformational isomers, is only 4.9 kcal/mol higher in energy than triplet (*Z*)-DMKC. Therefore, some of the excess energy is used for excitation into the singlet state; after that it is downhill to DMK, since the molecule still has more than enough energy to overcome the small singlet activation barrier.

TABLE 1: Product Absorptions (cm^{-1}) Observed in the Photolysis ($\lambda \geq 280$ nm) of Ar/Ozone/DMA (200/1/1) Mixtures

$^{16}O_3$/DMA/Ar O_3 54% photolyzed	rel intensity	$^{18}O_3$/DMA/Ar O_3 65% photolyzed	rel intensity	assignment	$^{16}O_3$/DMA/Ar O_3 54% photolyzed	rel intensity	$^{18}O_3$/DMA/Ar O_3 65% photolyzed	rel intensity	assignment
2901.7	1.3	2901.5	3.0	DMK	1362.0		1361.1		
2898.6		2897.7			1356.3[a]	3.4	1356.2[a]	8.5	
2344.2	98.8	2308.8	97.1	CO_2	1355.2	3.5	1355.8	4.5	BDN
2149.3	7.4	2092.9	4.2	monomeric CO	1353.1	4.6			MVK
2146.5	8.2			?	1337.7	0.6	1330.6	0.8	DMK
2142.3	14.2	2122.6	7.6	ketene	1330.3[a]	1.8			
2138.2	25.6	2086.2	25.7	CO aggregate	1328.4[a]				
2135.2					1296.1	1.4			ketoketene?
		2119.9	9.7	?	1251.6	5.0	1248.1	8.6	MVK
		2115.6	19.2	?			1239.5	5.9	
2129.7	100	2109.4	100	DMK			1236.7		
2126.7		2104.8					1223.0	4.3	
2119.5		2100.7			1241.1	0.6			MVK
2104.0	2.1	2081.1	7.9	ketoketene?	1224.8	1.0			AAH
2065.4	1.5			DMK	1183.8	13.6	1187.1	23.6	MVK
2064.0							1184.2		
1912.8	2.2						1179.2		
1885.6	1.1	1885.2	2.1				1149.9	0.5	
1882.6							1127.3	4.5	
1880.2					1129.1	7.1	1122.7	8.2	AAH/BDN
1851.6	4.3	1811.7	2.9	AAH	1120.5[a]	3.7	1119.7[a]	9.0	
1847.4					1065.5	1.4			
1805.0	0.9			AAH	1056.2[a]	0.5			
1771.3	6.5	1770.6	5.8	AAH			1098.5	1.4	
		1767.8					1089.7	4.7	
		1741.6	20.0		1004.6	1.1			MVK/DMK/AAH
		1739.3							
1740.8[a]	5.5	1707.4[a]	5.4	possibly band	997.0	11.5			MVK/DMK/AAH
1737.8[a]		1705.1[a]		observed by	992.2				
				DeMore[b]	987.3				
1726.6	24.9	1692.7	9.9		969.0	4.5	968.9	4.5	MVK
1723.6	24.0	1689.6	29.7	BDN	954.4	7.2	953.6	7.9	MVK
		1702.0	4.7	?			951.8		
1720.2	24.1	1695.5	25.6	(*Z*)-MVK			906.0	5.8	
		1681.5	4.1	?	939.3	1.2			MVK
1700.8	17.9	1670.7	13.2	(*E*)-MVK	935.4				
1696.8					912.5	2.1			AAH
1623.7	11.6	1617.8	8.2	MVK	729.0	0.5			DMK
1621.6							721.1	0.7	
		1599.5	3.5				702.9	0.9	
1454.6	0.5			DMK			695.4	0.7	
1433.7	0.4			MVK			686.8	2.1	
1425.5	4.2	1424.4	9.4	MVK	670.5	3.3	657.3	2.4	MVK
1404.3	2.1			MVK	667.5				
1399.1	13.1	1398.7	17.6	MVK			642.1	0.5	
1388.8	2.1	1388.5	3.1				637.3	0.8	
1379.2	2.5	1367.6	4.0	ketene	652.0	0.6			
1368.1	0.4			AAH	540.4[a]	2.0	528.9[a]	1.8	
1364.6	9.8	1363.6	23.7	MVK			520.7	1.5	

[a] This set of bands had an unusual set of growth kinetics in that they reached a maximum intensity at 10 min of photolysis time and decayed to near zero intensity at 120 min. [b] DeMore, W. B.; Lin, C-L. *J. Org. Chem.* **1973**, *38*, 985.

The activation energy required to convert triplet (*Z*)-DMKC from the ground state to singlet DMK is 6.8 kcal/mol. Triplet (*E*)-DMKC does not rearrange to triplet DMK because of conformational constraints within the molecule; i.e., the orbitals holding the lone electrons on the carbene carbon are pointing away from the methyl group which is to undergo an electrophilic 1,2 shift.

We next consider the formation of (*Z*)-methyl vinyl ketone ((*Z*)-MVK) from hot (*Z*)-DMKC. Plotted in Figure 4 is a potential energy diagram for the thermal rearrangement of triplet (*Z*)-DMKC to triplet (*Z*)-MVK, and for the thermal rearrangement of singlet DMKC to (*Z*)-MVK. The activation energy on the triplet surface is 45.5 kcal/mol; on the singlet surface it is 1.7 kcal/mol. While it is not impossible for this molecule to pass through the triplet transition state, it is unlikely. There is a near degeneracy in the energy of triplet (*Z*)-DMKC and fully optimized singlet DMKC at the third step in the reaction surface. Therefore, intersystem crossing to singlet DMKC and conversion to (*Z*)-MVK should be quite facile in this case. The minimum energy needed to convert triplet (*Z*)-DMKC to singlet (*Z*)-MVK is 6.6 kcal/mol.

The formation of (*E*)-methyl vinyl ketone ((*E*)-MVK) from triplet (*E*)-DMKC is qualitatively similar to the system of Z isomers. Plotted in Figure 5 is the potential energy diagram for the thermal rearrangement of triplet (*E*)-DMKC to triplet (*E*)-MVK, and for the thermal rearrangement of singlet DMKC to (*E*)-MVK. The activation energy needed to cross from ground state (*E*)-DMKC to triplet (*E*)-MVK is 45.7 kcal/mol. While we have not computed the exothermicity of the reaction of $O(^3P)$ with DMA to form triplet (*E*)-DMKC, it can be estimated from

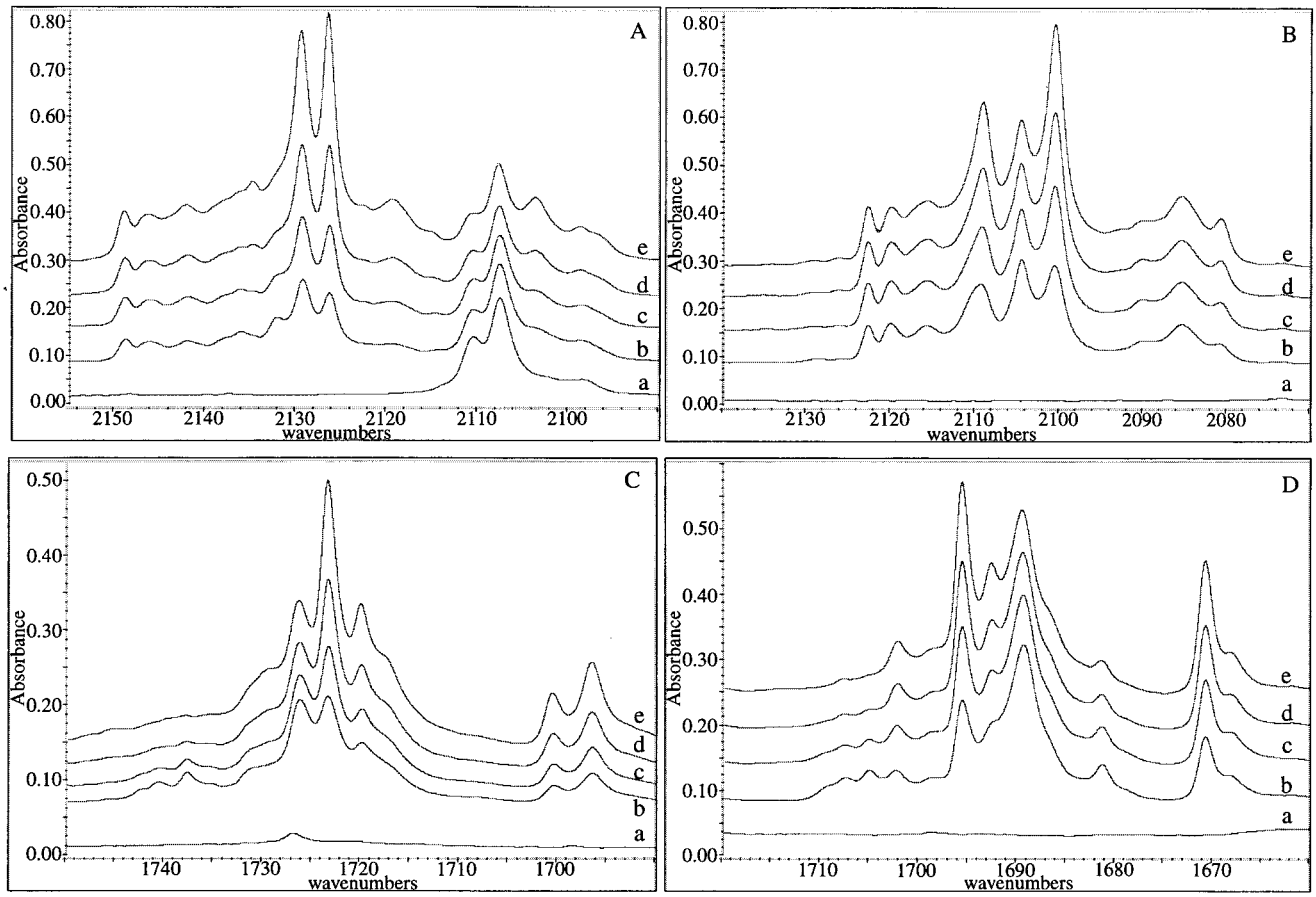

Figure 1. FTIR product bands in the ketene and carbonyl regions: (A) ^{16}O, (B) ^{18}O, (C) ^{16}O, (D) ^{18}O, (a) before photolysis, (b) 10 min photolysis, (c) 30 min, (d) 60 min, (e) 120 min.

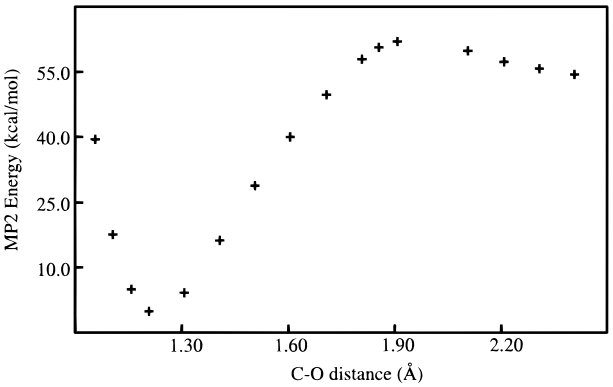

Figure 2. Plot of PMP2/6-31G(d,p) electronic potential energy vs C−O distance for the formation of triplet state (*Z*)-DMKC from DMA and O(^{3}P). The minimum occurs at $r = 1.2069$ Å; the transition state occurs at $r = 1.8537$ Å.

the relative energies of the E/Z forms of these isomers (Table 2), knowing that the energy released on forming (*Z*)-DMKC is 51.4 kcal/mol. We estimate that triplet (*E*)-DMKC is formed with 48.5 kcal/mol of excess energy. This amount of energy would be enough to cross the triplet state barrier to triplet (*E*)-MVK, but again, this would be unlikely since some of the energy of the molecule will be dissipated by collisions with the matrix. The minimum energy needed to cross from the ground state triplet (*E*)-DMKC to singlet (*E*)-MVK is 5.7 kcal/mol, assuming that the intersystem crossing point occurs early on the reactants side of the potential energy diagram.

We next consider the theoretical formation of dimethyloxirene (DMO) from triplet state (*E*)-DMKC. If formation of DMO could proceed on the triplet surface, (*E*)-DMKC would have to cross an activation barrier of 27.0 kcal/mol and then intersystem cross to singlet state DMO. However, this is unlikely because the excess energy of the energized (*E*)-DMKC will be rapidly dissipated by the matrix. It is more likely that (*E*)-DMKC will spin cross early on the reaction surface to the singlet state,

TABLE 2: Relative Energies of C_4H_6O Species

species [multiplicity]	rel energy (kcal/mol) UMP2	PMP2	CCSD(T)/6-31+G(d,p)// MP2/6-31+G(d,p)
(*E*)-DMKC [3]	72.2	67.4	65.7
(*Z*)-DMKC [3]	68.8	64.6	62.4
DMKC [1]	69.4	N/A	64.9
cis-DMO [3]	96.1	94.8	94.8
trans-DMO [3]	94.4	93.2	93.2
DMO [1]	63.8	N/A	65.8
(*E*)-MVK [3]	83.4	76.4	70.0
(*E*)-MVK [1]	0	N/A	0
(*Z*)-MVK [3]	82.3	75.3	68.9
(*Z*)-MVK [1]	0.10	N/A	0.048
DMK [3]	49.8	46.9	47.0
DMK [1]	5.7	N/A	8.1

TABLE 3: Activation Energies for Thermal Rearrangement of Triplet Dimethylketocarbenes to Singlet Products[a]

reaction [multiplicity]	E_a (kcal/mol) UMP2	PMP2	CCSD(T)
(*E*)-DMKC[3] → (*E*)-MVK[1]	0.91	5.7	6.6
(*Z*)-DMKC [3] → (*Z*)-MVK [1]	2.3	6.6	8.3
(*Z*)-DMKC [3] → DMK [1]	2.5	6.8	6.6
(*E*)-DMKC [3] → DMO [1]	−2.8	1.9	−1.0

[a] Activation energy is the difference between the transition state on the singlet surface and the ground-state triplet reactant.

TABLE 4: Activation Energies for Thermal Rearrangement of Dimethylketocarbenes to Isospin Products

	E_a (kcal/mol)		
reaction [multiplicity]	UMP2	PMP2	CCSD(T)
(*E*)-DMKC [3] → (*E*)-MVK [3]	46.0	45.7	46.9
(*Z*)-DMKC [3] → (*Z*)-MVK [3]	45.6	45.5	46.8
(*Z*)-DMKC [3] → DMK [3]	57.8	57.3	58.7
(*E*)-DMKC [3] → *trans*-DMO [3]	23.6	27.0	28.8
DMKC [1] → (*E*)-MVK [1]	3.7	NA	7.3
DMKC [1] → (*Z*)-MVK [1]	1.7	NA	5.8
DMKC [1] → DMK [1]	1.9	NA	4.1
DMKC [1] → DMO [1]	0.05	NA	−1.3
O(^{3}P) + DMA → (*Z*)-DMKC [3]	16.5[c]	8.0[a]	6.2[b]

[a] These energies were obtained from an MP2/6-31G(d,p) calculation. [b] CCSD(T)/6-31G(d,p)//MP2/6-31G(d,p) single-point calculation.

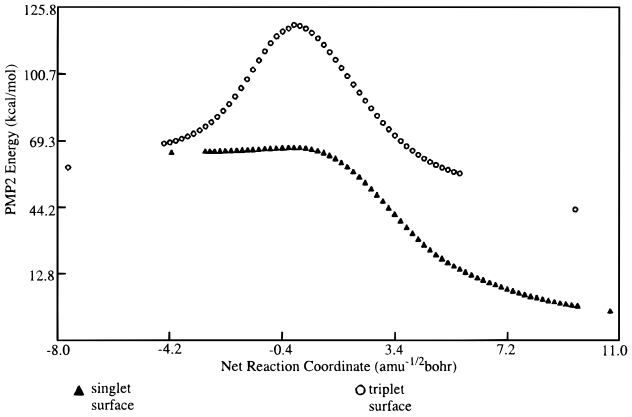

Figure 3. Potential energy diagram for the isomerization of triplet state (*Z*)-DMKC to triplet state DMK, and for the isomerization of singlet state DMKC to singlet state DMK. (*E*)-DMKC does not isomerize to DMK due to steric constraints within the molecule, see text.

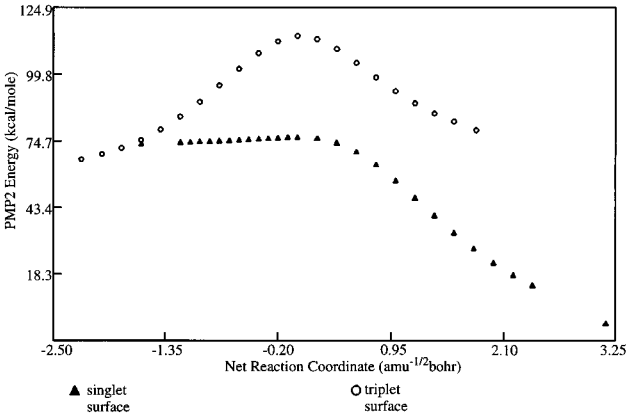

Figure 4. Potential energy diagram for the isomerization of triplet state (*Z*)-DMKC to triplet state (*Z*)-MVK, and for the isomerization of singlet state DMKC to singlet state (*Z*)-MVK.

whereby it will only have to cross a barrier of 1.9 kcal/mol, and come to rest 3.6 kcal/mol lower in energy than the triplet (*E*)-DMKC. We have not observed any evidence in the infrared spectrum for the formation of DMO under our experimental conditions. A possible reason for this is that the back reaction, DMO to singlet DMKC, would require only 5.65 kcal/mol of energy, at the MP2 level. Therefore, if the molecule still has sufficient energy when it reaches the DMO structure, it could return again to DMKC and then convert to DMK or MVK. It is more energetically favorable for DMKC to convert to DMK or MVK where the exothermicity of these reactions is on the order of 65 kcal/mol. Furthermore, we note that the triplet state

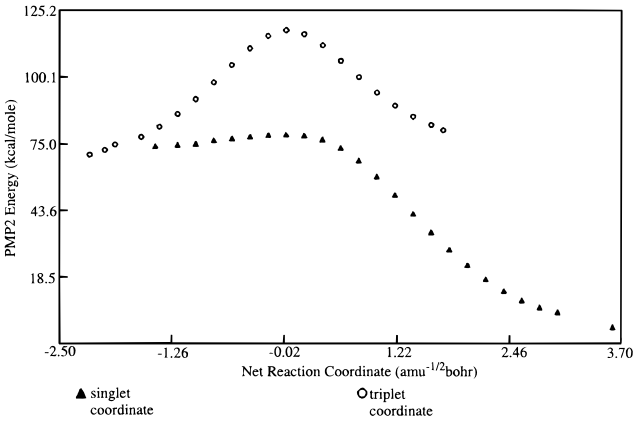

Figure 5. Potential energy diagram for the isomerization of triplet state (*E*)-DMKC to triplet state (*E*)-MVK, and for the isomerization of singlet state DMKC to singlet state (*E*)-MVK.

(*E*)-DMKC to singlet state DMO reaction is endothermic when considering the single-point CCSD(T) energies of Table 2. Considering that the activation barrier of this reaction is near zero, it would then become impossible to observe DMO. Tables 2, 3, and 4 summarize all of the results of our computational work for C_4H_6O species.

Dimethyloxirene has been observed by Bodot et al.[5,6] to form via photodissociation (broadband photolysis, $\lambda > 230$ nm) of N_2 from 3-diazo-2-butanone, trapped in either argon or krypton marices (M/R = 2000/1) at 20 K. While it may be possible for DMO to form under these conditions, we would like to address some aspects of Bodot's own data which suggest that his infrared assignment of the C═C symmetric stretching band of DMO, in the range 2131−2140 cm^{-1}, may be in error. Because of the symmetric nature of this molecule, the C═C symmetric stretch is expected to have a near-zero infrared absorption intensity. We have calculated the intensity of this mode to be 0.0125 km/mol at the MP2/6-31G(d,p) level. DMK, also a product of this photodissociation, has been assigned a C═C═O antisymmetric stretch in the range 2131.0−2120.5 cm^{-1}; its calculated infrared absorption intensity is 470 km/mol at the MP2/6-31G(d,p) level. Bodot's integrated absorbance data is 0.039 cm^{-1} for the ketene mode and 0.015 cm^{-1} for the oxirene mode. Using Beer's law and the calculated intensities, we find the concentration ratio of DMO/DMK to be 14 500/1. The concentration ratio seems extraordinarily high when the following is considered: DMK is 58.1 kcal/mol more stable than DMO (Table 2), and the activation energies for conversion of singlet DMKC to DMK and for conversion of singlet DMKC to DMO are both very low (Table 4). (The slight negative activation energy for the latter process at the single-point CCSD-(T) level is probably due to the fact that these structures have not been optimized at this level.) Furthermore, these workers failed to account for bands belonging to CO, a known photolysis product of dimethylketene, with a strong absorption at 2137 cm^{-1} in argon. We also find it curious that the other assigned bands of DMO have far weaker absorptions than the one assigned to the symmetric C═C stretch. While we are not stating that the Bodot assignment is conclusively in error, we believe it is important to consider the above points when assessing the DMO assignment. The uncertainties in the Bodo et al. assignment could be remedied by performing the same experiment with pure ^{18}O labeled 3-diazo-2-butanone. Bands due to carbon monoxide and dimethylketene would shift to 2100 cm^{-1} and lower, while the C═C stretch of dimethyloxirene would remain virtually unchanged. If weak bands were still observed in the 2131 to 2140 cm^{-1} range, this would be substantial evidence

for the observation of dimethyloxirene. The calculated infrared absorption intensities at this level of theory can be off by as much as a factor of 10; however, we believe that the magnitude of the concentration ratio is supportive of our conclusions.

Butane-2,3-dione. The only product with molecular formula $C_4H_6O_2$ resulting from the photolytic reaction of ozone and DMA is butane-2,3-dione (BDN). This product most likely forms as a result of reaction between singlet state oxygen molecules and DMA. The primary processes in ozone photolysis[32] in the 280−611 nm range are

$$O_3(^1A) \rightarrow O_2(^1\Delta_g) + O(^1D) \qquad \lambda \leq 310.0 \text{ nm} \qquad (1)$$

$$O_2(^3\Sigma_g^-) + O(^1D) \qquad \lambda \leq 411.0 \text{ nm} \qquad (2)$$

$$O_2(^1\Sigma_g^+) + O(^3P) \qquad \lambda \leq 463.0 \text{ nm} \qquad (3)$$

$$O_2(^1\Delta_g) + O(^3P) \qquad \lambda \leq 611.0 \text{ nm} \qquad (4)$$

When radiation is filtered through a 280 nm cutoff filter, process 1 should dominate because it is spin allowed; and, most of the oxygen atoms produced initially will be ^1D. Argon is known to be an effective quencher[32] of $O(^1D)$ and many of these atoms will go on to react as $O(^3P)$. However, the $O_2(^1\Delta_g)$ molecules are especially stable since, in order to relax to the ground state, they must spin cross to the triplet state and change angular momentum to the Σ state. Both of these processes are forbidden by selection rules. Therefore, we believe some of the $O_2(^1\Delta_g)$, and to a lesser extent $O_2(^1\Sigma_g^+)$, will survive to react with DMA.

In order to test this hypothesis, matrices were formed which contained Ar/DMA/O_2 in mole ratio of 200/1/1. The positions of the DMA absorbance peaks in this initial FTIR spectrum were shifted to 2976.3, 2936.8, 2872.6, 2740.9, 2056.4, 1447.2, 1407.1, 1404.3, 1378.9, 1157.9, 1131.4, 1039.3, and 1035.0 cm^{-1}. Assuming that the matrix is formed from a completely randomized distribution of atoms and molecules, and that DMA and O_2 occupy lattice sites that result from cubic close packing[33] (face-centered cubic unit cell) where the number of nearest neighbors is 12, then the probability[34] that DMA has one O_2 molecule as a nearest neighbor is 0.057. Upon photolysis of this matrix at $\lambda \geq 280$ nm and 20 min exposure time, no new bands were observed. We conclude from this observation that nearest-neighbor triplet state oxygen molecules do not react under these conditions. This observation is strongly supportive of the singlet oxygen molecule mechanism for the formation of BDN.

Next, the matrix was successively photolyzed for 30 min using only the water filter; under these conditions $\lambda > 220$ nm. Two very small bands appeared at 2149.0 and 2137.9 cm^{-1} with integrated absorbances of 0.055 and 0.063 cm^{-1}; these bands correspond to monomeric and aggregated carbon monoxide, respectively. No other product bands appeared under these conditions. Next, the matrix was annealed to 26 K. There was a slight increase in intensity of baseline CO_2 peaks near 2344 cm^{-1} and a simultaneous decrease in intensity of both CO peaks, indicating that some of the CO was oxidized to CO_2 by molecular oxygen. Under these conditions, small molecules such as oxygen and CO can diffuse through the matrix. It is notable that the O_2 molecules did not react with DMA as they did with CO. Only when the matrix was subjected to the full, unfiltered radiation of the lamp did other new product bands form. After 45 min of unfiltered irradiation, the matrix temperature rose to 28.2 K, large amounts of CO_2 and CO formed, and new bands corresponding to BDN appeared at 1722.8, 1354.8, 1121.2, and 541.5 cm^{-1}. Many other new bands also appeared: 2989.6, 1727.2, 1721.0, 1694.6, 1680.1, 1672.0, 1499.6, 1467.2, 1374.8, 1363.0, 1357.0, 1303.9, 1256.6, 1222.3, 1208.1, 923.0, 914.5, 867.1, 828.8, 821.5, 626.6, and 554.3 cm^{-1}; these bands have not been assigned.

We postulate that the BDN is formed by reaction of singlet oxygen molecules with DMA due to the following observations: ground state O_2 molecules did not react with DMA when the Ar/DMA/O_2 matrix was photolyzed using the 280 nm cutoff filter, nor did they react when the matrix was annealed; BDN did form when the Ar/DMA/O_3 matrix was photolyzed at $\lambda \geq 280$ nm. In order to explain the reaction between O_2 and DMA under the conditions where $\lambda > 220$ nm and $T = 28$ K, a mechanism analogous to the Kautsky mechanism[35] of dye-sensitized photooxygenations can be employed. O_2 is known to enhance reversibly radiative $S_0 \rightarrow T_1$ transitions in organic molecules. Therefore, it may be possible for some of the DMA to reach the triplet state via interaction with triplet O_2 and absorption of a photon near 220 nm. Once the triplet state is reached in DMA, electronic excitation energy is transferred from triplet DMA to triplet oxygen, generating singlet state DMA and singlet state oxygen (either $^1\Sigma_g^+$ or $^1\Delta_g$, depending on the amount of energy transferred). Now the singlet state oxygen molecules react with the DMA to form BDN.

$C_4H_6O_3$ and Products of Other Composition. The only observed product with molecular formula $C_4H_6O_3$ is acetic anhydride. This product most probably forms from photolysis of DMA/O_3 reactant pairs, or weak molecular complexes, since it has already been established that $O(^3P)$ and $^1O_2$ react facilely with DMA. It is interesting to note that, in the gas phase, acetic anhydride is not an observed product of the ozonolysis of DMA[36] when the ambient pressures are low to moderate (about 1 atm). Only when the pressure is increased to 100−300 psi is acetic anhydride observed. At moderate pressures the main products of this reaction are acetic acid and ketene. The formation of these products has been explained by the decomposition of highly energized acetic anhydride. In the matrix, we observe small amounts of ketene but no acetic acid. Therefore, the acetic anhydride must be stabilized by collisions with the matrix as it is formed. The observation of ketene can be explained by the photolytic decomposition of BDN, which was observed on photolysis of matrices containing Ar/BDN (1000/1) at $\lambda \geq 280$ nm.

An alternative explanation regarding the formation of acetic anhydride is one in which the intermediate ketocarbene triplet state is "trapped" by a triplet state oxygen molecule to form an α-carbonyl carbonyl oxide:

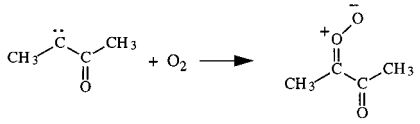

This type of structure has been proposed[37] to be an intermediate in the Criegee mechanism of alkyne ozonation. There is indirect evidence for the apparent existence of this species from the reactivity of an unidentified intermediate formed from 2-butyne and ozone at −70 °C in CH_2Cl_2.[38] Addition of alkenes to this mixture produced epoxides in 10−12% yield. The authors concluded that the most likely mechanism for the formation of the epoxide was oxygen atom transfer from the α-carbonyl carbonyl oxide. We have performed a geometry optimization and normal vibrational mode analysis of this α-carbonyl carbonyl oxide at the MP2/6-311G(d,p) level of theory. The three strongest, unscaled normal modes of this molecule with their corresponding infrared intensities are 1181.8 cm^{-1}, 102.7

SCHEME 1: Schematic Diagram of Observed Matrix Reactions When 200/1/1:Ar/Ozone/DMA Matrices Are Irradiated with Photons of $\lambda \geq 280$ nm

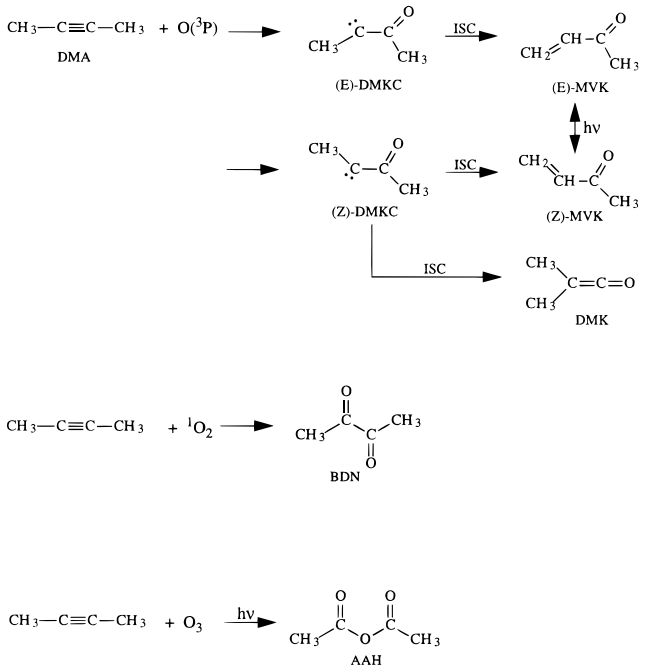

km/mol; 1135.9 cm^{-1}, 525.5 km/mol; and 899.1 cm^{-1}, 869.4 km/mol. Undoubtedly, the strong intensities of these bands reflect the large degree of charge separation in this molecule. We have searched for the spectroscopic signature of this molecule in our infrared matrix spectra and have not been able to find it. The species is formed in too low a concentration to be detected, or it rearranges immediately to acetic anhydride, photolyzes to BDN and oxygen atoms, or it is not formed at all.

The observed band at 2104.0 cm^{-1} (Table 1) is too low in frequency to be attributed to dimethylketene. It is possible, however, that this absorption is due to a ketoketene species, $CH_3(C{=}C{=}O)(C{=}O)CH_3$, which results from trapping of the intermediate ketocarbene by carbon monoxide—present in the matrix due to photodecomposition of dimethylketene and BDN. CO_2 formation in the matrix can be attributed to oxidation of carbon monoxide by ozone and other oxidants such as O_2.

Finally, there is a strong band which forms in the carbonyl region at 1726.6 cm^{-1} which we have been unable to assign to any of the aforementioned products. In the reaction of $^1O_2$ with DMA, a strong carbonyl absorption was observed at 1727.2 cm^{-1}. It is possible that these two bands are the same band due to the same species. A summary of the observed matrix reactions is given in Scheme 1.

V. Conclusions

The reaction of $O(^3P)$ with dimethylacetylene in argon matrices at 12 K produces dimethylketene and the E/Z configurational isomers of methyl vinyl ketone. The initial "product" of reaction is triplet state dimethylketocarbene, which intersystem crosses "early" on the reaction surface, to take advantage of the low singlet activation barriers, and form the above stable products. The E/Z configurational isomers of methyl vinyl ketone interconvert via photon absorption at $\lambda \geq 280$ nm. No infrared product absorption bands could be assigned to dimethyloxirene. Dimethylacetylene reacts with singlet state O_2, generated via photolysis of ozone, to form butane-2,3-dione. Dimethylacetylene/O_3 reactant pairs photolyze to form acetic anhydride.

Acknowledgment. Partial support from the National Science Foundation through OSR-9452857, the Office of Naval Research through grant N00614-93-1-0079, and the Mississippi Center for Supercomputing Research is gratefully acknowledged.

References and Notes

(1) Hucknall, D. J. *Chemistry of Hydrocarbon Combustion*; Chapman and Hall: London, 1985.
(2) Wayne, R. P. *Chemistry of Atmospheres*, 2nd ed.; Oxford University Press: Oxford, UK; 1991.
(3) Lippard, S. J.; Berg, J. M. *Principles of Bioinorganic Chemistry*; University Science Books: Mill Valley, CA.
(4) Haller, I.; Pimentel, G. C. *J. Am. Chem. Soc.* **1962**, *84*, 2855.
(5) Debû, F.; Monnier, M.; Verlaque, P.; Davidovics, G.; Pourcin, J.; Bodot, H.; Aycard, J.-P. *C. R. Acad. Sc. Paris, t. 303, Sér. II* **1986**, *10*, 897.
(6) Bachmann, C.; N¢Guessan, T. Y.; Debû, F.; Monnier, M.; Pourcin, J.; Aycard, J.-P., Bodot, H. *J. Am. Chem. Soc.* **1990**, *112*, 7488. Scott, A. P.; Nobes, R. H.; Schaefer, III, H. F.; Radom, L. *J. Am. Chem. Soc.* **1994**, *116*, 10159.
(7) Fowler, J. E.; Galbraith, J. M.; Vacek, G.; Schaefer, III, H. F. *J. Am. Chem. Soc.* **1994**, *116*, 9311.
(8) Vacek, G.; Galbraith, J. M.; Yamaguchi, Y.; Schaefer, III, H. F., Nobes, R. H.; Scott, A. P.; Radom, L. *J. Phys. Chem.* **1994**, *98*, 8660−8665.
(9) Wolff, L. *Justus Liebigs Ann. Chem.* **1912**, *394*, 23.
(10) Csizmadia, I. G.; Font, J.; Strausz, O. P. *J. Am. Chem. Soc.* **1968**, *90*, 7360.
(11) Torres, M.; Bourdelande, J. L.; Clement, A.; Strausz, O. P. *J. Am. Chem. Soc.* **1983**, *105*, 1698.
(12) Mahaffy, P. G.; Visser, D.; Torres, M.; Bourdelande, J. L.; Strausz, O. P. *J. Org. Chem.* **1987**, *52*, 2680.
(13) Tomoika, H.; Okuno, H.; Izawa, Y. *J. Org. Chem.* **1980**, *45*, 5278. Tomoika, H.; Kondo, M.; Izawa, Y. *J. Org. Chem.* **1981**, *46*, 1090.
(14) McMahon, R. J.; Chapman, O. L. Hayes, R. A.; Hess, T. C. Krimmer, H-P. *J. Am. Chem. Soc.* **1985**, *107*, 7597.
(15) DeMore, W. B.; Raper, O. F. *J. Chem. Phys.* **1966**, *44*, 1780.
(16) Liu, L.; Davis, S. R. *J. Phys. Chem.* **1992**, *96*, 9719.
(17) *Gaussian 94*, Revision E.3, Frisch, M. J.; Trucks, G. W.; Schlegel, H. B.; Gill, P. M. W.; Johnson, B. G.; Robb, M. A.; Cheeseman, J. R.; Keith T.; Petersson, G. A.; Montgomery, J. A.; Raghavachari, K.; Al-Laham, M. A.; Zakrzewski, V. G.; Ortiz, J. V.; Foresman, J. B.; Cioslowski, J.; Stefanov, B. B.; Nanayakkara, A.; Challacombe, M.; Peng, C. Y.; Ayala, P. Y.; Chen, W.; Wong, M. W.; Andres, J. L.; Replogle, E. S.; Gomperts, R.; Martin, R. L.; Fox, D. J.; Binkley, J. S.; Defrees, D. J.; Baker, J.; Stewart, J. P.; Head-Gordon, M.; Gonzalez , C.; Pople, J. A. Gaussian, Inc.: Pittsburgh, PA, 1995.
(18) Moller, C.; Plesset, M. S. *Phys. Rev.* **1934**, *46*, 618.
(19) Dithcfield, R.; Hehre, W. J.; Pople, J. A. *J. Chem. Phys.* **1971**, *54*, 724.
(20) Hariharan, P. C.; Pople, J. A. *Theor. Chim. Acta* **1973**, *28*, 213.
(21) McLean, A. D.; Chandler, G. S. *J. Chem. Phys.* **1980**, *72*, 5639.
(22) Krishnan, R.; Binkley, J. S.; Seeger, R.; Pople, J. A. *J. Chem. Phys.* **1980**, *72*, 650.
(23) Cizek, J. *Adv. Chem. Phys.* **1969**, *14*, 35.
(24) Purvis, G. D.; Bartlett, R. J. *J. Chem. Phys.* **1982**, *76*, 1910.
(25) Scuseria, G. E.; Janssen, C. L.; Schaefer, III, H. F. *J. Chem. Phys.* **1988**, *89*, 7382.
(26) Scuseria, G. E.; Schaefer, III, H. F. *J. Chem. Phys.* **1988**, *90*, 3700.
(27) Pople, J. A.; Head-Gordon, M.; Raghavachari, K. *J. Chem. Phys.* **1987**, *87*, 5968.
(28) Collins, S. *J. Phys. Chem.* **1985**, *89*, 845.
(29) Fletcher, W. H.; Barish, W. B. *Spectrochim. Acta* **1965**, *21*, 1647.
(30) Moore, C. B.; Pimentel, G. C. *J. Chem. Phys.* **1963**, *38*, 2816.
(31) Leroi, G. E.; Ewing, G. E.; Pimentel, G. C. *J. Chem. Phys.* **1964**, *8*, 2298.
(32) Okabe, H. *Photochemistry of Small Molecules*; John Wiley and Sons: New York, 1978.
(33) Meyer, B. *Low-Temperature Spectroscopy*; American Elsevier Publishing Co., Inc.: New York, 1971.
(34) Bandow, H.; Akimoto, H. *J. Phys. Chem.* **1985**, *89*, 845.
(35) Kautsky, H. *Trans. Faraday Soc.* **1939**, *35*, 216.
(36) DeMore, W. B. *Int. J. Chem. Kinet.* **1971**, III, 161.
(37) Criegee, R.; Lederer, M. *Justus Liebigs Ann. Chem.* **1953**, *583*, 29.
(38) Keay, R. E.; Hamilton, G. A. *J. Am. Chem. Soc.* **1975**, *97*, 6876.